Magnetic Coupling and Optical Properties of the S-6- Dodecakis(trifluoromethyl) fullerene Radical Anions in the Layered Salt (PPN+)[C-60(CF3)(12)]

ARTICLE *in* CHEMISTRY - A EUROPEAN JOURNAL · APRIL 2014

Impact Factor: 5.73 · DOI: 10.1002/chem.201304850 · Source: PubMed

6 AUTHORS, INCLUDING:

Dmitri V Konarev
Russian Academy of Sciences
171 PUBLICATIONS **1,921** CITATIONS
SEE PROFILE

Alexey A Goryunkov
Lomonosov Moscow State University
72 PUBLICATIONS **859** CITATIONS
SEE PROFILE

Rimma Nikolaevna Lyubovskaya
Russian Academy of Sciences
450 PUBLICATIONS **3,708** CITATIONS
SEE PROFILE

ChemPubSoc Europe

DOI: 10.1002/chem.201304850

CHEMISTRY
A European Journal
Full Paper

Fullerenes

Magnetic Coupling and Optical Properties of the S_6-Dodecakis(trifluoromethyl)fullerene Radical Anions in the Layered Salt $(PPN^+)[C_{60}(CF_3)_{12}^{\bullet-}]$**

Dmitri V. Konarev,*[a] Natalia A. Romanova,[b] Roman A. Panin,[b] Alexey A. Goryunkov,[b] Sergey I. Troyanov,[b] and Rimma N. Lyubovskaya[a]

Abstract: Poly(trifluoromethyl)fullerene S_6-$C_{60}(CF_3)_{12}$ was reduced by sodium fluorenone ketyl in the presence of (PPN)Cl (PPN = bis(triphenylphosphine)iminium) to afford the salt $(PPN)[C_{60}(CF_3)_{12}]$ (**1**), which contains $C_{60}(CF_3)_{12}^{\bullet-}$ radical anions. In the crystal structure of **1**, $C_{60}(CF_3)_{12}^{\bullet-}$ layers alternate with the PPN^+ cations. There are short F···F contacts between $C_{60}(CF_3)_{12}^{\bullet-}$ radical anions within the layers but no C···C contacts. DFT calculations revealed that the negative charge on $C_{60}(CF_3)_{12}^{\bullet-}$ is distributed mainly between sp^2 carbon and fluorine atoms, whereas spin density is localized mainly on the fullerene-cage sp^2 carbon atoms. IR and UV/Vis/NIR spectra in the solid state and solution showed characteristic changes relative to those of neutral S_6-$C_{60}(CF_3)_{12}$ due to the formation of radical anions. The solid-state electronic spectrum of **1** exhibits a single broad band at 738 nm attributed to $C_{60}(CF_3)_{12}^{\bullet-}$. Crystals of **1** show a narrow EPR signal with $g = 2.0025$ ($\Delta H = 0.45$ mT) at 300 K. The temperature dependence of the integral intensity follows the Curie–Weiss law with a negative Weiss temperature of −11.8 K (30–300 K) indicating antiferromagnetic interaction of spins. This dependence was approximated by the Heisenberg model for one-dimensional chains of antiferromagnetically interacting spins with exchange interaction $J/k_B = -9.1$ K. It was assumed that magnetic interaction between the $C_{60}(CF_3)_{12}^{\bullet-}$ spins in the layers is mediated by short F···F contacts.

Introduction

Compounds containing ionic fullerene moieties attract much attention due to properties such as one-, two-, and three-dimensional metallic conductivity,[1–3] superconductivity,[3,4] and ferromagnetic ordering.[5] This interest was also extended to fullerene derivatives in which addends are attached to the fullerene core. However, only a few compounds containing ionic fullerene derivatives were obtained and characterized in the solid state.[6–15]

The most studied fullerene polyadducts are fluoro-, bromo-, and chlorofullerenes.[16,17] However, bromo- and chlorofullerenes decompose during reduction and therefore cannot form stable ionic compounds.[18,19] Fullerene derivatives in which addends are linked to the fullerene core by C–C bonds generally form more stable anions, and in some cases ionic compounds with promising physical properties can be obtained. For example, the reduction of $C_{60}[CH(m\text{-}NO_2Ph)]$ and $C_{60}[CH(m\text{-}NH_2Ph)]$ by cobaltocene allows the preparation of ionic $(C_{60}[CHAr]^{\bullet-})(Cp_2Co^+)$ complexes with full charge transfer, as follows from optical spectra.[6–8] Magnetic measurements on both complexes revealed ferromagnetic ordering of spins below 19 K. Such behavior is unusual, since the Cp_2Co^+ cations are diamagnetic, so that magnetism can be only attributed to spins localized on the fullerene derivatives. It was shown that the spins in the ferromagnetic $(TDAE^{\bullet+})(C_{60}^{\bullet-})$ are localized on both $C_{60}^{\bullet-}$ and $TDAE^{\bullet+}$ (TDAE = tetrakis(dimethylamino)ethylene).[5] Crystal structures of the above complexes are unknown, and this hampers the explanation of their magnetic behavior. Ionic $(C_{60}[CHAr]^{\bullet-})(Cp_2Co^+)$ complexes with NO_2 or NH_2 groups in *ortho* or *para* positions of the phenyl ring exhibit only antiferromagnetic interaction of spins down to 4 K. Similar behavior is observed in ionic complexes of $C_{60}[C(COOEt)_2]$ and $C_{70}[C(COOEt)_2]$ with cobaltocene and TDAE.[6,7] Several ionic complexes were synthesized with dicyanofullerene $C_{60}(CN)_2$, which can be more easily reduced than C_{60}.[9] It forms ionic complexes and salts with bis(benzene)chromium $[Cr^0(C_6H_6)_2]$, cobaltocene, and potassium cations in the presence of dibenzo-18-crown-6.[10,11] The structure of the $C_{60}(CN)_2^{\bullet-}$ radical anion was determined in the ionic multicomponent compound $[Cr^I(C_6H_6)_2^{\bullet+}]_2[Co^{II}TPP\{C_{60}(CN)_2^-\}][C_{60}(CN)_2^{\bullet-}]$ (TPP = tetraphenylporphyrin).[12] Weak antiferromagnetic interaction was observed

[a] Dr. D. V. Konarev, Prof. R. N. Lyubovskaya
Institute of Problems of Chemical Physics RAS
Chernogolovka, 142432 (Russia)
Fax: (+7) 496-522-18-52
E-mail: konarev@icp.ac.ru

[b] Dr. N. A. Romanova, R. A. Panin, Dr. A. A. Goryunkov, Prof. S. I. Troyanov
Chemistry Department
Lomonosov Moscow State University,
Leninskie Gory, Moscow, 119991 (Russia)

[**] PPN^+: bis(triphenylphosphine)iminium.

Supporting information for this article is available on the WWW under http://dx.doi.org/10.1002/chem.201304850.

below 50 K in polycrystalline ionic compound ($TDAE^{\bullet+}$)($DP3FP^{\bullet-}$), in which DP3FP is *cis*-2′,5′-bis(pyridin-3-yl)pyrrolidino[3′,4′:1,9][60]fullerene.[13] Two ionic complexes of fullerene penta-adducts potassium pentaphenylfullerenide and pentakis(biphenyl-4-yl)fullerenide coordinated by 18-crown-6 or THF were isolated and studied by X-ray crystallography.[14,15] However, the fullerenide anions do not contain unpaired electrons and both compounds are diamagnetic. Thus, it can be summarized that only fullerene derivatives containing one, two, or five addends were previously used for the preparation of ionic compounds, and most of them were obtained as polycrystalline samples.

Nowadays, the chemistry of trifluoromethyl derivatives of C_{60}, C_{70}, and higher fullerenes is being progressively developed. More than a hundred derivatives have been structurally characterized, and electrochemical behavior and optical properties of some of them have been studied.[20–25] Moreover, some of these derivatives undergo reversible electrochemical reduction to mono-, di-, and trianionic states without loss of addends.[25] Therefore, they are potentially suitable for the preparation of ionic compounds. Although most trifluoromethyl fullerenes can be isolated only in very small quantities,[20–25] a few of them, for example, dodecakis(trifluoromethyl)fullerene, S_6-$C_{60}(CF_3)_{12}$, are accessible in gram quantities.[26,27]

Here we report the isolation of the salt of the S_6-$C_{60}(CF_3)_{12}^{\bullet-}$ radical anion with the bis(triphenylphosphine)iminium cation (PPN^+), which was characterized by X-ray crystallography, optical and magnetic studies. This is the first solid-state study on a radical anion of a highly functionalized fullerene derivative with twelve bulky addends. Moreover, this salt shows strong magnetic coupling of spins in spite of shielding of the fullerene carbon cage by trifluoromethyl groups. These results demonstrate that ionic compounds containing polyfunctionalized fullerenes can exhibit promising magnetic properties.

Results and Discussion

Synthesis

The S_6-$C_{60}(CF_3)_{12}$ molecule has a specific addition pattern with all CF_3 groups attached in alternating *para* and *meta* positions in the near-equatorial belt of edge-sharing hexagons leaving two opposing triphenylene moieties on the poles (Figure 1). The addition of twelve acceptor CF_3 groups to the fullerene core could be expected to increase the acceptor ability of S_6-$C_{60}(CF_3)_{12}$. However, this compound is a weaker electron acceptor than pristine C_{60} by about −0.16 V, and its first reduction potential is about −0.60 V versus SCE.[25] The second reduction potential of $C_{60}(CF_3)_{12}$ (hereafter, the prefix S_6 is omitted for brevity) was theoretically estimated to be −0.58 V versus $C_{60}^{0/-}$ (ca. −1.02 V vs. SCE).[25] TDAE as a strong donor (the first oxidation potential is −0.75 V vs. SCE[28]) easily reduces fullerene C_{60} to the radical anion state, but C_{60}^{2-} dianions do not form even with a large excess of TDAE.[29] A suspension of $C_{60}(CF_3)_{12}$ (20 mg) in *o*-dichlorobenzene (*o*-DCB) does not react with an excess of TDAE (0.5 mL). Pristine $C_{60}(CF_3)_{12}$, which is sparingly soluble in *o*-DCB, could be recovered by slow diffusion of hexane into the filtered solution. Decamethylchromocene (Cp^*_2Cr) and decamethylcobaltocene (Cp^*_2Co) are stronger donors with first oxidation potentials at −1.04 and −1.55 V versus SCE,[30] respectively, and therefore are able to reduce $C_{60}(CF_3)_{12}$. As a result of reduction, 20 mg of $C_{60}(CF_3)_{12}$ dissolved completely in 14 mL of *o*-DCB with formation of green and blue solutions after treatment with Cp^*_2Cr and Cp^*_2Co, respectively. Most probably, reduction of $C_{60}(CF_3)_{12}$ to the mono- and dianionic states takes place, as can be deduced by comparing the oxidation potentials of these donors with the first and second reduction potentials of $C_{60}(CF_3)_{12}$. Slow precipitation of the complexes by diffusion of hexane resulted in the formation of green and gray noncrystalline powders.

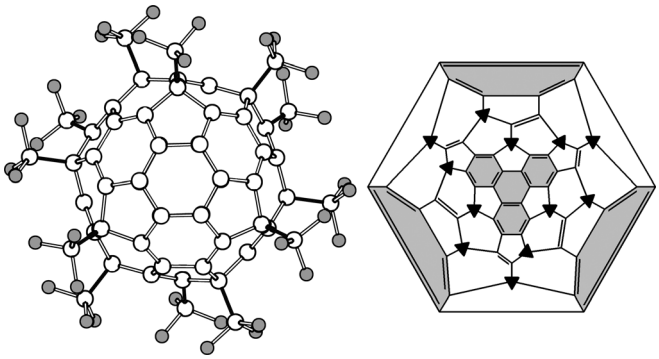

Figure 1. The S_6-$C_{60}(CF_3)_{12}$ molecule viewed along S_6 axis and its Schlegel diagram. The attachment positions of the CF_3 groups are marked by black triangles; the triphenylene moieties are highlighted in gray.

Reduction of $C_{60}(CF_3)_{12}$ by an excess of sodium fluorenone ketyl in *o*-DCB in the presence of large organic PPN^+ cations was also accompanied by complete dissolution of $C_{60}(CF_3)_{12}$ and the formation of green solution of the monoanions. Two-month diffusion of hexane resulted in crystallization of the salt $(PPN^+)\{C_{60}(CF_3)_{12}^{\bullet-}\}$ (**1**) as black, well-shaped blocks. In contrast, the reduction of fullerenes C_{60} and C_{70} with sodium fluorenone ketyl in the presence of PPN^+ under similar experimental conditions led to the dianionic states, and $(PPN^+)_2(C_{60}^{2-})$ and $(PPN^+)_2(C_{70}^{2-})$ salts solvated by *o*-DCB were isolated.[31,32] Thus, $C_{60}(CF_3)_{12}$ is a weaker acceptor than C_{60} and is reduced to the monoanion only at potentials close to the second reduction potential of C_{60} ($E^{-/2-} = -0.66$ to −0.83 V vs. SCE in different solvents[33]).

Optical spectra of $C_{60}(CF_3)_{12}$ mono- and dianions

Optical spectra of mono- and dianions of $C_{60}(CF_3)_{12}$ were recorded in *o*-DCB solution. Monoanions were produced by reduction with sodium fluorenone ketyl in the presence of (PPN)Cl with formation of a green solution, as described above. Dianions were generated by reduction of $C_{60}(CF_3)_{12}$ with 2.1 equivalents of Cp^*_2Co with formation of a blue solution. The same spectrum was observed at a larger excess of Cp^*_2Co, that is, Cp^*_2Co is unable to reduce $C_{60}(CF_3)_{12}$ to the trianionic state. The reduction of $C_{60}(CF_3)_{12}$ to mono- and dianionic states is accompanied by the appearance of new broad bands at

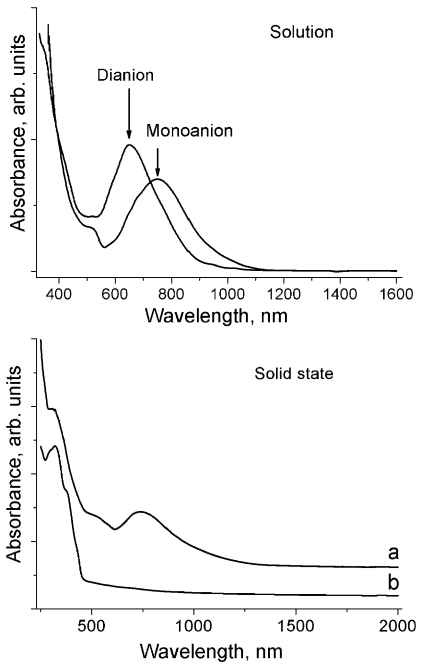

Figure 2. Top: UV/Vis/NIR spectra of monoanions and dianions of $C_{60}(CF_3)_{12}$ in *o*-DCB solution. Bottom: Solid-state UV/Vis/NIR spectra of a) salt **1** and b) pristine S_6-$C_{60}(CF_3)_{12}$ in KBr pellets. Solution and solid-state spectra of **1** were recorded under anaerobic conditions.

750 nm (1.65 eV) and 648 nm (1.91 eV), respectively (Figure 2, top). Note that the absorption band of dianions is shifted to higher energies relative to that of monoanions. Therefore, as in the case of C_{60},[29,30] the charged state of $C_{60}(CF_3)_{12}$ can be easily determined on the basis of Vis/NIR spectra.

Solid-state spectra of salt **1** and parent $C_{60}(CF_3)_{12}$ in KBr pellets are shown in Figure 2 (bottom). $C_{60}(CF_3)_{12}$ shows absorption only up to 460 nm, whereas salt **1** shows broad absorption in the whole visible range with a maximum at 738 nm (1.68 eV). The position of this band is close to that in the solution spectrum of $C_{60}(CF_3)_{12}^{\bullet-}$ (750 nm) and is consistent with the monoanionic state of $C_{60}(CF_3)_{12}$ in salt **1**. Mono- and dianions of $C_{60}(CF_3)_{12}$ have absorption bands at higher energies than C_{60} (main bands at 1070–1080 nm (1.16–1.15 eV) and 943–952 nm (1.31–1.30 eV), respectively).[33,34]

Similarly, additional blueshifted absorption bands were reported to appear in the electronic spectra of electrochemically generated $C_{60}(CF_3)_2^{\bullet-}$ (932 and 1516 nm), $C_{60}(CF_3)_2^{2-}$ (880 and 1336 nm), and $C_{60}(CF_3)_{10}^{\bullet-}$ (isomer 3, 565 and 828 nm).[35] The monoanions of pyridine-substituted fulleropyrrolidine in the solid-state spectrum of $(TDAE^{\bullet+})(DP3FP^{\bullet-})$ and dicyanofullerene in *N*,*N*-dimethylformamide solution exhibit absorption bands at 998 nm (1.24 eV)[13] and 1019 nm (1.22 eV),[10] respectively.

Infrared spectrum of $C_{60}(CF_3)_{12}^{\bullet-}$

The IR spectrum of pristine $C_{60}(CF_3)_{12}$ contains several very strong absorption bands at 1160–1260 cm^{-1} attributed to the stretching vibrations of the CF_3 groups, and other bands are observed at 1110, 1079, 1009, 988, 940, 886, 793, 767, 758, 743, 737, 714, 679, 604, and 518 cm^{-1} (Table S1 and Figure S1 in the Supporting Information).[26] The main absorption bands of $C_{60}(CF_3)_{12}^{\bullet-}$ in **1** at 743 and 758 cm^{-1} are shifted by 3–5 cm^{-1} to the red. The largest redshifts of 8–10 cm^{-1} are observed for strong absorption bands at 940, 988, and 1009 cm^{-1}. Noticeable changes are observed for characteristic absorption bands of the CF_3 groups in the 1160–1260 cm^{-1} range. Strong bands at 1223 and 1246 cm^{-1} disappear, and the absorption bands at 1180 and 1200 cm^{-1} are redshifted by 3–6 cm^{-1}.

The redshifts of both the C–C vibrations of the cage and the C–F vibrations suggest that the negative charge of $C_{60}(CF_3)_{12}^{\bullet-}$ is mainly localized on these fragments and results in the elongation of some C–C and C–F bonds. These redshifts are in accordance with the previously reported IR spectra of the radical anions of fullerene derivatives. The absorption bands of $C_{60}(CN)_2$ attributed to the C≡N vibrations are redshifted from 2241 to 2230 and 2233 cm^{-1} in the spectra of ionic $(Cr^{I}(C_6H_6)_2^{\bullet+})_2\{Co^{II}TPP[C_{60}(CN)_2^{-}]\}[C_{60}(CN)_2^{\bullet-}]$[12] and $(Cp_2Co^{+})[C_{60}(CN)_2^{\bullet-}]$,[10] respectively. The formation of $C_{60}^{\bullet-}$ and negatively charged fullerene derivatives is also accompanied by redshifts (by 30–40 cm^{-1}) of the absorption bands attributed to the C–C vibrations of the fullerene core at 1420–1430 cm^{-1}.[13,33,34]

Crystal structure of $(PPN^{+})[C_{60}(CF_3)_{12}^{\bullet-}]$

In the crystal structure of **1**, the asymmetric unit contains two halves of $C_{60}(CF_3)_{12}^{\bullet-}$ and one PPN^{+} cation, and thus a stoichiometric 1:1 composition results. One half of $C_{60}(CF_3)_{12}^{\bullet-}$ is well ordered with only one of six CF_3 groups exhibiting librational disorder. Another crystallographically independent half of $C_{60}(CF_3)_{12}^{\bullet-}$ is statistically disordered between two orientations with occupancies of 0.7608/0.2392(16). A $C_{60}(CF_3)_{12}^{\bullet-}$ layer parallel to the *ac* plane and the projection of the crystal structure along the *a* axis are shown in Figures 3 and 4, respectively. Intermolecular distances were calculated for the main orientation of one $C_{60}(CF_3)_{12}^{\bullet-}$ moiety only.

The crystal structure of **1** is composed of layers of $C_{60}(CF_3)_{12}^{\bullet-}$ radical anions parallel to the *ac* plane (Figure 3). In the *b* direction, the layers are separated by bulky PPN^{+} cations. Crystalline $C_{60}(CF_3)_{12}$ has a columnar arrangement of the molecules with a short distance of 3.316 Å between the pole hexagons of adjacent molecules, which is typical for stacking interactions between flat aromatic molecules. As a result, the interfullerene center-to-center distance is very short (9.716 Å).[26] In the crystal structure of **1**, the arrangement of $C_{60}(CF_3)_{12}^{\bullet-}$ anions is quite different. The pole hexagons of the neighboring $C_{60}(CF_3)_{12}^{\bullet-}$ radical anions are widely spaced, so that no stacking interaction exists. The distances between the centers of fullerene cages in the layers are 11.8 Å along the *a* axis and 12.2 Å along the *c* axis. The center-to-center distances of 14.5 Å between fullerene moieties of different layers are longer. There are several short van der Waals (vdW) F···F contacts between $C_{60}(CF_3)_{12}^{\bullet-}$ units along the *a* and *c* axes (six such contacts exist for each $C_{60}(CF_3)_{12}^{\bullet-}$ radical anion in the range of 2.791–2.853 Å; see Figure 3). The F···F distances along the *b* axis are slightly longer (>2.96 Å). In addition, there are

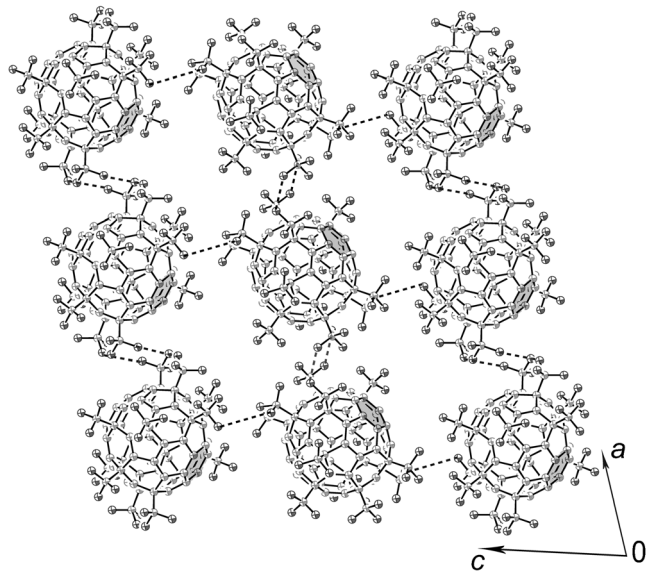

Figure 3. $C_{60}(CF_3)_{12}^{\bullet-}$ layer parallel to the *ac* plane. The F···F contacts shorter than the sum of the vdW radii of two F atoms (2.94 Å) are shown by dashed lines. Central hexagons of triphenylene substructures of $C_{60}(CF_3)_{12}^{\bullet-}$ are highlighted in gray.

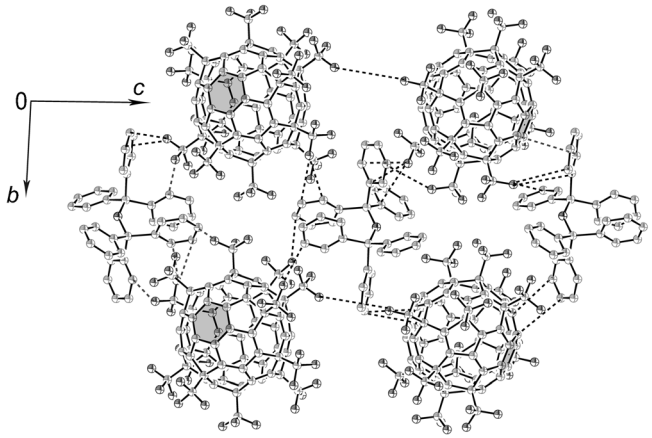

Figure 4. Crystal structure of **1** viewed along the *a* axis. The layers of $C_{60}(CF_3)_{12}^{\bullet-}$ units in the *ac* plane are separated by PPN^+ cations. The vdW F···F contacts between $C_{60}(CF_3)_{12}^{\bullet-}$ and C···F contacts between $C_{60}(CF_3)_{12}^{\bullet-}$ and PPN^+ are shown by dashed lines. The central hexagons of the triphenylene substructures of $C_{60}(CF_3)_{12}^{\bullet-}$ are highlighted in gray.

multiple short F···C(PPN^+) and F···H(PPN^+) contacts with phenyl groups of PPN^+ (Figure 4).

Average bond lengths in $C_{60}(CF_3)_{12}^{\bullet-}$ were calculated for the ordered molecule only. The average lengths of double (sp^2–sp^2), and single C–C cage bonds of 1.372(3) and 1.436(3) Å, respectively, are very close to the average lengths of these type of bonds in the neutral $C_{60}(CF_3)_{12}$ molecule (1.373(1) and 1.438(1) Å, respectively).[26] The average C–CF_3 and C–F bond lengths in the radical anion of 1.535(3) and 1.325(3) Å are slightly shorter than similar bonds in neutral $C_{60}(CF_3)_{12}$ (1.542(1) and 1.332(1) Å, respectively).[26] However, the observed shortening of 0.007 Å is within the experimental error. Thus, we can conclude that no noticeable changes in bond lengths are observed on formation of $C_{60}(CF_3)_{12}^{\bullet-}$ from neutral $C_{60}(CF_3)_{12}$. Most probably, delocalization of negative charge over a great number of C–C and C–F bonds results in very small changes in the bond lengths which cannot be evidenced reliably at the attained accuracy of the X-ray data. The $C_{60}(CF_3)_{12}^{\bullet-}$ radical anion is slightly elongated along the poles; the interplane distance between two opposite hexagons at the poles increases from 6.400 Å in the neutral state to 6.440 Å in the radical-anion state. Similar elongation of spherical C_{60} (0.02–0.04 Å) is observed in its mono- and dianions due to the Jahn–Teller effect.[31]

Theoretical calculations

The molecular and electronic structures of the $C_{60}(CF_3)_{12}^{\bullet-}$ radical anion were calculated at the DFT level of theory with PBE exchange-correlation functional and TZ2P basis set.[36] According to the data obtained, the radical anion preserves the S_6 symmetry of the neutral molecule with only minor changes in the bond lengths of 0.001–0.007 Å (see Table 1 and Figure 5).

Table 1. Average experimental and DFT calculated (in brackets) bond lengths of $C_{60}(CF_3)_{12}$ in neutral and monoanionic states.

Bond type[a]	Bond lengths [Å]		
	Neutral[26]	Anion	Difference
	Double C(sp^2)–C(sp^2)		
a	1.357(1) [1.361]	1.355(3) [1.365]	−0.002 [0.004]
f	1.370(1) [1.374]	1.363(3) [1.378]	−0.007 [0.004]
d	1.374(1) [1.383]	1.379(3) [1.390]	0.005 [0.007]
i	1.391(1) [1.404]	1.395(3) [1.403]	0.004 [−0.001]
	Single C–C		
e	1.422(1) [1.422]	1.424(3) [1.427]	0.002 [0.005]
c	1.427(1) [1.432]	1.433(3) [1.427]	0.006 [−0.005]
g	1.429(1) [1.431]	1.430(3) [1.436]	0.001 [0.005]
b	1.465(1) [1.464]	1.454(3) [1.458]	−0.011 [−0.006]
h	1.449(1) [1.450]	1.446(3) [1.447]	−0.003 [−0.003]
	C–CF_3		
I	1.538(1) [1.564]	1.532(3) [1.558]	−0.006 [−0.007]
II	1.546(1) [1.566]	1.540(3) [1.564]	−0.006 [−0.002]
	C–F		
	1.332(1) [1.355]	1.325(3) [1.359]	−0.007 [0.004]

[a] Bond notations are shown in Figure 5.

The theoretical bond lengths are systematically overestimated by 0.001–0.016 Å for both neutral and negatively charged $C_{60}(CF_3)_{12}$. Similar to the experimental data, equatorial (I) and near-pole (II) C–CF_3 bonds are shortened by 0.007 and 0.002 Å, respectively, whereas C–F bonds are slightly elongated (by 0.003–0.005 Å). The changes in the bond lengths of C–C double and single bonds of the fullerene cage are within 0.001–0.007 Å, in compliance with experimentally observed values (0.001–0.011 Å). The changes in the distances between the opposite carbon atoms of the fullerene cage vary slightly from 0.03 to −0.02 Å. A comparison between experimental dis-

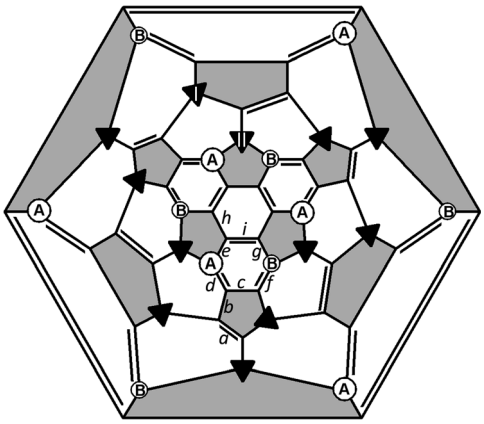

Figure 5. Schlegel diagram of $C_{60}(CF_3)_{12}^{\bullet-}$ with notations of C–C bonds and sites with maximal charge and spin density localization (circles labeled A and B). Black triangles denote the positions of the attached CF_3 groups.

tances along the S_6 axis for neutral and monoanionic $C_{60}(CF_3)_{12}$ (6.400 and 6.440 Å) and those predicted by DFT (6.423 and 6.426 Å, respectively) demonstrates that the predicted values are overestimated for the neutral state and underestimated for the anion. The possible reasons for this inconsistency are the neglect of short stacking interactions in crystalline $C_{60}(CF_3)_{12}$ and ionic interactions in the salt **1**. Thus, DFT calculations did not show any significant change in molecular geometry and bond lengths as a result of the formation of $C_{60}(CF_3)_{12}^{\bullet-}$.

Atomic partitions of charge and spin density were calculated according to the Hirschfeld method (Table 2).[36] Drawings of the DFT-predicted LUMO for $C_{60}(CF_3)_{12}$ are given in the Supporting information (Figure S2). Negative charge is distributed

Table 2. DFT calculated[a] atomic partitions of charge and spin density in $C_{60}(CF_3)_{12}^{\bullet-}$.

Atoms[b]	Net charge density[c]		Spin density	
	total	per atom	total	per atom
sp^2 C_A	−0.10	−0.016	0.27	0.044
sp^2 C_B	−0.08	−0.013	0.17	0.029
sp^2 C_{rest}	−0.34	−0.009	0.40	0.011
sp^3 C_{cage}	−0.03	−0.002	0.06	0.005
sp^3 $C(F_3)$	−0.06	−0.005	0.08	0.007
F	−0.40	−0.011	0.03	0.001

[a] PBE/TZ2P charge and spin densities are given according to the Hirschfeld method.[36] [b] Atom labeling is shown in Figure 5. [c] Net charge density was determined as the difference in atomic partitions of charge density of $C_{60}(CF_3)_{12}$ in monoanionic and neutral forms.

mainly between sp^2 carbon atoms (−0.5 e) and fluorine atoms (−0.4 e). The maximal charge partition values per atom were found for 12 sp^2 carbon atoms of types A and B (−0.016 e and −0.013 e per atom, respectively) surrounding the central hexagon of the triphenylene-like moiety (Figure 5). The average charge for the remaining 36 sp^2 carbon atoms is −0.009 e per atom. Such charge localization is consistent with a LUMO density distribution in $C_{60}(CF_3)_{12}^{\bullet-}$ (Supporting Information, Figure S2). Spin density is localized on the fullerene-cage sp^2 carbon atoms (0.84) with the maximal spin-density at sp^2 carbon atoms of types A and B (0.044 and 0.029 per atom, respectively). Much lower spin density is distributed over fluorine atoms, 0.03 in total or 0.001 per F atom.

The hyperfine coupling constants a_F for fluorine atoms were estimated from spin-density values at the fluorine nuclei. The calculated a_F values of 0.002 and 0.006 mT for two different type of fluorine atoms (average values for each of two types of CF_3 groups) are too low to be resolved in EPR spectra.

EPR spectra and magnetic properties

Salt **1** shows a narrow EPR signal at 300 K, which can be fitted well by one Lorentzian line with $g = 2.0025$ and a line width of $\Delta H = 0.41$ mT (Figure 6). Integral intensity of this signal approximately corresponds to the contribution of one $S = 1/2$ spin per formula unit. This signal can be unambiguously attributed to the $C_{60}(CF_3)_{12}^{\bullet-}$ radical anions, since the PPN^+ cations are diamagnetic and EPR-silent. Generally, the presence of addends substantially reduces fullerene symmetry and removes the orbital degeneracy. As a result, the g factors of the EPR signals of

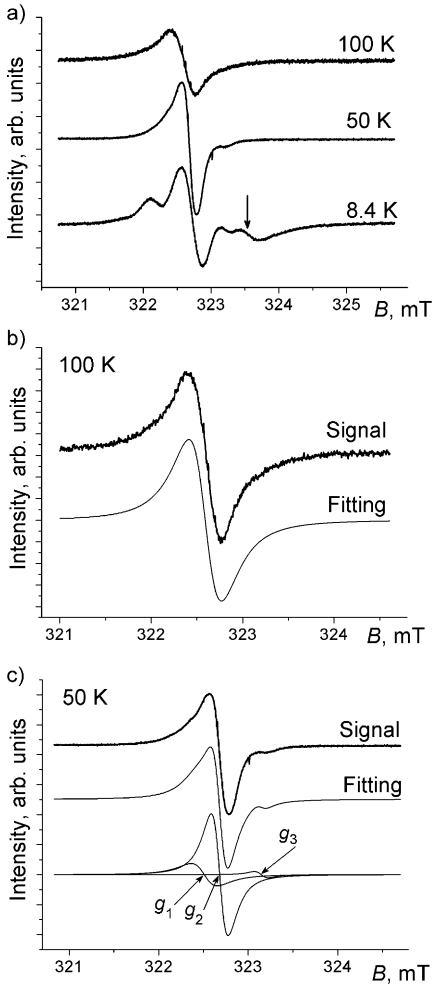

Figure 6. a) Evolution of the EPR spectrum of **1** with decreasing temperature from 100 down to 8.4 K; intensity is not normalized. Fitting of the EPR signal of **1** at 100 (b) and 50 K (c) by one and three Lorentzian lines, respectively.

the radical anions of fullerene derivatives move closer to $g=2.0023$ and the signals are narrowed relative to those of $C_{60}^{\bullet-}$. For instance, paramagnetic $(C_{60}^{\bullet-})_2$ dimers bonded by two C–C bonds exhibit a doublet-like EPR signal with $g=2.0014$ and a line width of 0.315 mT at room temperature.[37] Electrochemically generated $C_{60}(CF_3)_2^{\bullet-}$ and $C_{60}(CF_3)_{10}^{\bullet-}$ (isomer 3) radical anions show g factors of 2.0016 and 2.0032, respectively,[35] whereas the $DP3FP^{\bullet-}$ radical anions in $(TDAE^{\bullet+})(DP3FP^{\bullet-})$ show an asymmetric EPR signal with $g_1=2.0030$ ($\Delta H=0.7$ mT) and $g_2=2.0035$ ($\Delta H=0.5$ mT) at room temperature (these two signals can originate from different paramagnetic $DP3FP^{\bullet-}$ and $TDAE^{\bullet+}$ species).[13] Most radical anions of fullerene derivatives generated in solution also show narrow EPR signals with g factors greater than 2.0000.[38–40]

The EPR signal shows nearly temperature independent g factor and line width in the 300–100 K range. The signal deviates from the Lorentzian shape below this temperature (Figure 7, T_1), but it can be satisfactorily fitted by two Lorentzian lines with $g_1=2.0022$ ($\Delta H=0.45$ mT) and $g_2=2.0016$ ($\Delta H=0.21$ mT) at 90 K. The intensity of the g_2 signal is higher than that of the g_1 signal. A new lower-field component is observed below 60 K (Figure 7, T_2), and this signal can be fitted by three Lorentzian lines at 50 K: an intense component with $g_2=2.0016$ ($\Delta H=0.21$ mT) and two weaker components with $g_1=2.0025$ ($\Delta H=0.28$ mT) and $g_3=1.9986$ ($\Delta H=0.26$ mT) (Figure 6, spectrum at 50 K). A three-component signal is observed down to 4 K. However, signal intensity strongly decreases below 20 K. Below this temperature the g_1 and g_2 lines are noticeably shifted to higher and lower magnetic fields (Figure 7), so that one can observe more clearly the g_1 line on the background of the central g_2 line (Figure 6, spectrum at 8.4 K). The g_1 and g_2 lines are also broadened below 20 K. The decreased intensity of all three lines and the shifts in g factors of the g_1 and g_2 lines with decreasing temperature may be due to antiferromagnetic interaction of spins below 20 K. A new weak signal with $g=1.9967$ ($\Delta H=0.62$ mT) emerges below 10 K (Figure 7, T_3); it is indicated by an arrow in the spectrum of **1** at 8.4 K (Figure 6a). This weak signal does not exceed several percent of the intensity of the main signal at high temperatures and shows a purely paramagnetic temperature behavior down to 4 K. Therefore, it can be attributed to impurities. Probably, the observation of this signal became possible due to a significant decrease of the main signal below 20 K.

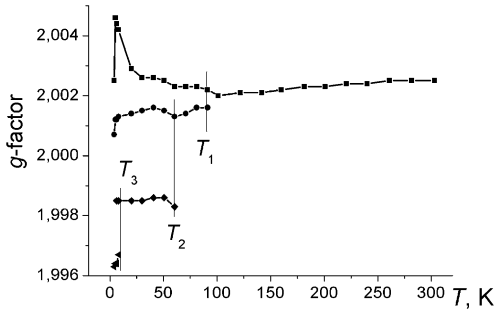

Figure 7. Temperature dependence of g factors of EPR signals of **1** in the 4–300 K range. T_1, T_2, and T_3 correspond to temperatures of signal splitting into two and three components and the appearance of a new signal with $g=1.996$–1.997, respectively.

The temperature dependence of the reciprocal integral intensity of the signal in the 4–300 K range is shown in Figure 8a. Its linearity in the 30–300 K range allows the determination of a Weiss temperature of −11.8 K, which indicates antiferromagnetic coupling of spins. Deviation from the Curie–Weiss law to antiferromagnetic behavior is observed below 20 K. The temperature dependence of integral intensity of the signal can also be well described in the 30–300 K range by the Curie–Weiss law with negative Weiss temperature of −11.8 K (Supporting information, Figure S3). Integral intensity of the signal decreases below 20 K, and the behavior of this system in the whole experimental temperature range can be well approximated by the Heisenberg model for one-dimensional chains of antiferromagnetically interacting spins[41] with exchange interaction of $J/k_B=-9.1$ K (Figure 8b). We also tried to fit the data using the Heisenberg models for antiferromagnetic interaction of spins in the isolated pairs or in the layers. However, the best fitting was observed in the model for antiferromagnetic interaction of spins in one-dimensional chains. Thus, the antiferromagnetic coupling between the $C_{60}(CF_3)_{12}^{\bullet-}$ spins that occurs in **1** is strong enough for it to show one-dimensional character.

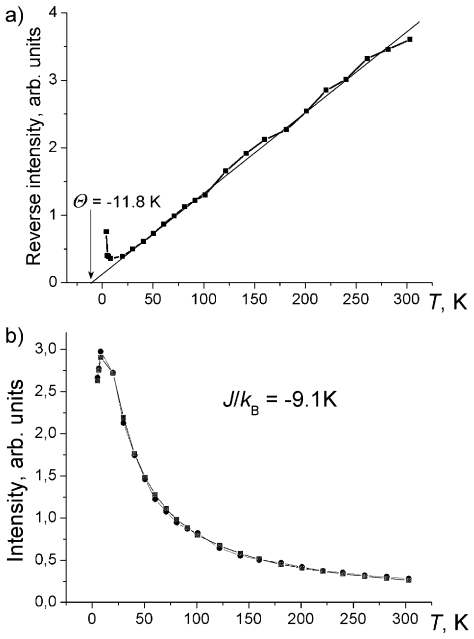

Figure 8. a) Temperature dependence of reciprocal intensity of the EPR signal; fitting of the dependence by the straight line revealed a Weiss temperature of −11.8 K. b) Approximation of the temperature dependence of integral intensity of EPR signal by the Heisenberg model for one-dimensional chains of antiferromagnetically interacting spins[41] with exchange interaction of $J/k_B=-9.1$ K.

As described above, the $C_{60}(CF_3)_{12}^{\bullet-}$ radical anions are arranged in two-dimensional layers with rather long distances between the fullerene cages (center-to-center distances of

about 12 Å). In the salts of C_{60} anions, such long interfullerene distances indicate packing of isolated fullerenes and the absence of magnetic interaction between $C_{60}^{\bullet-}$ radical anions, as evidenced by near-zero Weiss temperatures.[42–44] Whereas C···C contacts between the carbon cages are absent in **1**, short F···F vdW contacts are present. Moreover, these contacts are not uniform within the layers, since the shortest F···F contacts (2.79–2.80 Å) are found in the $C_{60}(CF_3)_{12}^{\bullet-}$ chains along the *a* axis. The IR spectroscopic data and DFT calculations show that that negative charge and electron density of $C_{60}(CF_3)_{12}^{\bullet-}$ are partially localized on fluorine atoms of the CF_3 groups. Most probably, the network of close F···F contacts is responsible for magnetic coupling of $C_{60}(CF_3)_{12}^{\bullet-}$ in the layers.

Conclusion

Dodecakis(trifluoromethyl)fullerene, S_6-$C_{60}(CF_3)_{12}$, was found to be a weaker acceptor than C_{60}. Its reduction to the mono- and dianionic states is only possible by using strong reducing agents. For the first time, the salt of an anionic multiply derivatized fullerene, namely, $(PPN^+)[C_{60}(CF_3)_{12}^{\bullet-}]$ (**1**), was obtained as single crystals by reduction with sodium fluorenone ketyl. According to X-ray crystallography, radical anions of $C_{60}(CF_3)_{12}^{\bullet-}$ in salt **1** are arranged in layers with short F···F contacts between $C_{60}(CF_3)_{12}^{\bullet-}$ moieties. DFT calculations showed that negative charge density is distributed in $C_{60}(CF_3)_{12}^{\bullet-}$ mainly on sp^2 carbon and fluorine atoms, whereas spin density is localized on cage sp^2 carbon atoms. The $C_{60}(CF_3)_{12}^{\bullet-}$ radical anions exhibit a narrow EPR signal with $g = 2.0025$ at 300 K, which is characteristic of radical anions of various fullerene derivatives. Magnetic data indicate strong one-dimensional magnetic coupling between the $C_{60}(CF_3)_{12}^{\bullet-}$ spins, most probably due to partial localization of electron and spin density on fluorine atoms and mediation of the magnetic coupling through the network of short F···F contacts. Therefore, ionic compounds based on trifluoromethyl derivatives of fullerene can demonstrate promising magnetic properties. This work will be continued with other trifluoromethyl derivatives of C_{60} and C_{70}.

Experimental Section

Materials

PPNCl was purchased from Aldrich. Sodium fluorenone ketyl was obtained as previously described.[45] The solvents were degassed and stored in a glove box. *o*-Dichlorobenzene ($C_6H_4Cl_2$) was distilled over CaH_2 under reduced pressure, and hexane was distilled over Na/benzophenone. All manipulations for the synthesis of air-sensitive **1** were carried out in an MBraun 150B-G glovebox with controlled atmosphere and contents of H_2O and O_2 of less than 1 ppm. The crystals were stored in a glovebox and sealed under anaerobic conditions in 2 mm quartz tubes at 10^{-5} Torr for EPR measurements. KBr pellets for IR and UV/Vis/NIR measurements were prepared in a glove box.

General

UV/Vis/NIR spectra were measured on KBr pellets with a PerkinElmer Lambda 1050 spectrometer in the 250–2500 nm range. FTIR spectra were recorded on KBr pellets with a PerkinElmer Spectrum 400 spectrometer (400–7800 cm^{-1}). EPR spectra were recorded for a polycrystalline sample of **1** at 4–300 K with a JEOL JES-TE 200 X-band ESR spectrometer equipped with a JEOL ES-CT470 cryostat. We also tried to measure the magnetic susceptibility of **1** with a Quantum Design MPMS-XL SQUID magnetometer. However, the amount of **1** was not enough for precise measurements.

Synthesis

S_6-$C_{60}(CF_3)_{12}$: S_6-$C_{60}(CF_3)_{12}$ was synthesized by the reaction of C_{60} (100 mg, 0.139 mmol) with gaseous CF_3I (ca 1 mL, 12 mmol) at 420 °C in a three-section glass ampoule for 48 h, as described elsewhere.[26,27] Crude crystalline material was collected (170 mg, raw yield of 79%) and recrystallized from boiling *o*-DCB (180 °C) to give pure S_6-$C_{60}(CF_3)_{12}$ (120 mg, 55% yield). MS (MALDI): *m/z* (%): 1410.0 $[M-2CF_3]^-$ (31), 1479.0 $[M-CF_3]^-$ (100), 1548.0 $[M]^-$ (11); UV/Vis (*o*-DCB): $\lambda = 318$, 336 (sh), 378, 409 (sh), 427 nm.

Reduction of S_6-$C_{60}(CF_3)_{12}$: The experiments on the reduction of S_6-$C_{60}(CF_3)_{12}$ with strong donors such as TDAE, Cp^*_2Cr, and Cp^*_2Co were carried out in a glovebox in degassed *o*-DCB.

(PPN)[$C_{60}(CF_3)_{12}$] (1): $C_{60}(CF_3)_{12}$ (22 mg, 0.0142 mmol) and slight excess of PPNCl (10 mg, 0.0174 mmol) were stirred in *o*-DCB (14 mL) with excess of sodium fluorenone ketyl (5 mg, 0.0246 mmol) at 80 °C for 2 h. $C_{60}(CF_3)_{12}$ is very slightly soluble in *o*-dichlorobenzene even at 80 °C, forming a suspension in a light yellow solution. As a result of reduction, complete dissolution was observed with formation of a green solution. After cooling, the solution was filtered in a 50 mL glass tube of 1.8 cm in diameter with a ground glass plug, and 30 mL of hexane was layered over the solution. Crystals of the salt formed over two months as well-shaped black blocks. The solvent was decanted and the crystals were washed with hexane. Crystals with sizes up to $0.4\times0.4\times0.3$ mm were obtained in a yield of 14% (4 mg). The composition of **1** was determined by X-ray crystallography. Several selected crystals showed the same unit cell and composition and thus confirmed the phase purity of the reaction product.

Quantum chemical calculations

After preliminary optimization at the AM1 level of theory (see Supporting Information for details), S_6-$C_{60}(CF_3)_{12}$ and its radical anion $C_{60}(CF_3)_{12}^{\bullet-}$ were optimized at the DFT level (r.m.s. gradient 10^{-6} a.u. $Å^{-1}$) by using PRIRODA software[46] with the original TZ2P basis set and PBE exchange-correlation functional.[47] Atomic partitions of the charge and spin densities are given according to the Hirschfeld method.[36]

X-ray crystallography

Data for a crystal of **1** were collected with a Gemini-R CCD diffractometer by using monochromated $Mo_{K\alpha}$ radiation ($\lambda = 0.71073$ Å). The structure was solved by direct methods and refined by the full-matrix least-squares method against F^2 by using the SHELX-97 package.[48] Non-hydrogen atoms were refined in the anisotropic approximation. Positions of hydrogen atoms were included in the refinement by using a riding mode. There are two crystallographically independent halves of $C_{60}(CF_3)_{12}$ and one PPN moiety in the asymmetric unit. One of the halves of $C_{60}(CF_3)_{12}$ has one rotationally disordered CF_3 group with occupancies of 0.781/0.219(14), and the other has two orientations with occupancies of 0.7608/0.2392(16).

Crystal data for **1** at 100(2) K: $C_{108}H_{30}F_{36}NP_2$, $M_r = 2087.27$; black block; triclinic, $P\bar{1}$; $a = 11.8097(5)$, $b = 14.5028(6)$, $c = 24.3936(10)$ Å;

$\alpha = 79.243(3)$, $\beta = 77.960(4)$, $\gamma = 80.462(4)^\circ$; $V = 3979.2(3)$ Å^3; $Z = 2$; $\rho_{calcd} = 1.742$ g·cm^{-3}; $\mu = 0.199$ mm^{-1}; $F(000) = 2078$; $2\theta_{max} = 59.56^\circ$; 75267 measured reflections, 19909 unique reflections, 15209 reflections with $I > 2\sigma(I)$, 1570 parameters refined, 21 restraints; $R_1 = 0.0562$, $wR_2 = 0.1373$, GoF = 1.040. CCDC 974345 contains the supplementary crystallographic data for this paper. These data can be obtained free of charge from The Cambridge Crystallographic Data Centre via www.ccdc.cam.ac.uk/data_request/cif.

Acknowledgements

The work was supported by RFBR-JSPS grant No. 12-03-92107 (Japan-Russia Research Cooperative Program) and the Russian Foundation for Basic Research (grants 12-03-00324 and 12-03-31513).

Keywords: anions · density functional calculations · fullerenes · magnetic properties · radical ions

[1] P. W. Stephens, G. Bortel, G. Faigel, M. Tegze, A. Jánossy, S. Pekker, G. Oszlanyi, L. Forró, *Nature* **1994**, *370*, 636 – 639.
[2] D. V. Konarev, S. S. Khasanov, A. Otsuka, M. Maesato, G. Saito, R. N. Lyubovskaya, *Angew. Chem.* **2010**, *122*, 4939 – 4942; *Angew. Chem. Int. Ed.* **2010**, *49*, 4829 – 4832.
[3] K. Tanigaki, K. Prassides, *J. Mater. Chem.* **1995**, *5*, 1515 – 1527.
[4] A. Y. Ganin, Y. Takabayashi, P. Jeglič, D. Arčon, A. Potocnik, P. J. Baker, Y. Ohishi, M. T. McDonald, M. D. Tzirakis, A. McLennan, G. R. Darling, M. Takata, M. J. Rosseinsky, K. Prassides, *Nature* **2010**, *466*, 221 – 225.
[5] P. W. Stephens, D. Cox, J. W. Lauher, L. Mihaly, J. B. Wiley, P. M. Allemand, A. Hirsch, K. Holczer, Q. Li, J. D. Thompson, F. Wudl, *Nature* **1992**, *355*, 331 – 333.
[6] M. Mrzel, P. Umek, P. Cevk, A. Omerzu, D. Mihailovic, *Carbon* **1998**, *36*, 603 – 606.
[7] M. Mrzel, A. Omerzu, P. Umek, D. Mihailovic, Z. Jagličić, Z. Trontelj, *Chem. Phys. Lett.* **1998**, *298*, 329 – 334.
[8] D. Mihailovic, *Monatsh. Chem.* **2003**, *134*, 137 – 154.
[9] M. Keshavarz-K, B. Knight, G. Srdanov, F. Wudl, *J. Am. Chem. Soc.* **1995**, *117*, 11371 – 11372.
[10] Z. Suo, X. Wey, K. Zhou, Y. Zang, C. Li, Z. Xu, *J. Chem. Soc. Dalton Trans.* **1998**, 3875 – 3878.
[11] Y. Yoshida, A. Otsuka, O. O. Drozdova, K. Yakushi, G. Saito, *J. Mater. Chem.* **2003**, *13*, 252 – 257.
[12] D. V. Konarev, S. S. Khasanov, A. Otsuka, Y. Yoshida, G. Saito, *J. Am. Chem. Soc.* **2002**, *124*, 7648 – 7649.
[13] D. V. Konarev, S. S. Khasanov, A. B. Kornev, M. A. Faraonov, P. A. Troshin, R. N. Lyubovskaya, *Dalton Trans.* **2012**, *41*, 791 – 798.
[14] Y. Matsuo, K. Tahara, E. Nakamura, *Chem. Lett.* **2005**, *34*, 1078 – 1079.
[15] Y. Matsuo, E. Nakamura, *J. Am. Chem. Soc.* **2005**, *127*, 8457 – 8466.
[16] R. Taylor, In *The Chemistry of Fullerenes*, World Scientific Pub Co Inc, Singapore, New Jersey, London, Hong-Kong, **1995**.
[17] A. A. Goryunkov, N. S. Ovchinnikova, I. V. Trushkov, M. A. Yurovskaya, *Russ. Chem. Rev.* **2007**, *76*, 289 – 312.
[18] Y. Yoshida, A. Otsuka, O. O. Drozdova, G. Saito, *J. Am. Chem. Soc.* **2000**, *122*, 7244 – 7251.
[19] P. A. Troshin, O. A. Troshina, S. M. Peregudova, E. I. Yudanova, A. G. Buyanovskaya, D. V. Konarev, A. S. Peregudov, A. N. Lapshin, R. N. Lyubovskaya, *Mendeleev Commun.* **2006**, *16*, 206 – 208.
[20] D. V. Ignat'eva, I. N. Ioffe, S. I. Troyanov, L. N. Sidorov, *Russ. Chem. Rev.* **2011**, *80*, 631 – 647.
[21] E. I. Dorozhkin, D. V. Ignat'eva, N. B. Tamm, A. A. Goryunkov, P. A. Khavrel, I. N. Ioffe, A. A. Popov, I. V. Kuvychko, A. V. Streletskiy, V. Yu. Markov, J. Spandal, S. H. Strauss, O. V. Boltalina, *Chem. Eur. J.* **2006**, *12*, 3876 – 3889.
[22] E. I. Dorozhkin, A. A. Goryunkov, I. N. Ioffe, S. M. Avdoshenko, V. Yu. Markov, N. B. Tamm, D. V. Ignat'eva, L. N. Sidorov, S. I. Troyanov, *Eur. J. Org. Chem.* **2007**, 5082 – 5094.
[23] D. V. Ignat'eva, A. A. Goryunkov, I. N. Ioffe, L. N. Sidorov, *J. Phys. Chem. A* **2013**, *117*, 13009 – 13017.
[24] N. A. Romanova, M. A. Fritz, K. Chang, N. B. Tamm, A. A. Goryunkov, L. N. Sidorov, C. Chen, S. Yang, E. Kemnitz, S. I. Troyanov, *Chem. Eur. J.* **2013**, *19*, 11707 – 11716.
[25] A. A. Popov, I. E. Kareev, N. B. Shustova, E. B. Stukalin, S. F. Lebedkin, K. Seppelt, S. H. Strauss, O. V. Boltalina, L. Dunsch, *J. Am. Chem. Soc.* **2007**, *129*, 11551 – 11568.
[26] S. I. Troyanov, A. Dimitrov, E. Kemnitz, *Angew. Chem.* **2006**, *118*, 2005 – 2008; *Angew. Chem. Int. Ed.* **2006**, *45*, 1971 – 1974.
[27] N. A. Romanova, T. S. Papina, V. A. Luk'yanova, A. G. Buyanovskaya, R. M. Varuschenko, A. I. Druzhinina, A. A. Goryunkov, V. Yu. Markov, R. A. Panin, L. N. Sidorov, *J. Chem. Thermodyn.* **2013**, *66*, 59 – 64.
[28] K. Kuwata, D. H. Geske, *J. Am. Chem. Soc.* **1964**, *86*, 2101 – 2105.
[29] D. V. Konarev, N. V. Drichko, A. Graja, *J. Chim. Phys.* **1998**, *95*, 2143 – 2156.
[30] J. L. Robbins, N. Edelstein, B. Spencer, J. C. Smart, *J. Am. Chem. Soc.* **1982**, *104*, 1882 – 1893.
[31] D. V. Konarev, A. V. Kuzmin, S. V. Simonov, E. I. Yudanova, S. S. Khasanov, G. Saito, R. N. Lyubovskaya, *PhysChemChemPhys* **2013**, *15*, 9136 – 9144.
[32] D. V. Konarev, S. I. Troyanov, S. S. Khasanov, A. Otsuka, H. Yamochi, G. Saito, R. N. Lyubovskaya, *Asian J. Chem.* **2013**, *8*, 1139 – 1143.
[33] C. A. Reed, R. D. Bolskar, *Chem. Rev.* **2000**, *100*, 1075 – 1120.
[34] D. V. Konarev, R. N. Lyubovskaya, *Russ. Chem. Rev.* **2012**, *81*, 336 – 366.
[35] A. A. Popov, J. Tarábek, I. E. Kareev, S. F. Lebedkin, S. H. Strauss, O. V. Boltalina, L. Dunsch, *J. Phys. Chem. A* **2005**, *109*, 9709 – 9711.
[36] F. L. Hirshfeld, *Theor. Chim. Acta* **1977**, *44*, 129 – 138.
[37] D. V. Konarev, S. S. Khasanov, A. Otsuka, G. Saito, H. Yamochi, R. N. Lyubovskaya, *New J. Chem.* **2011**, *35*, 1829 – 1835.
[38] P. Boulas, F. D'Souza, C. C. Henderson, P. A. Cahill, M. T. Jones, K. M. Kadish, *J. Phys. Chem.* **1993**, *97*, 13435.
[39] V. Brezová, A. Staško, P. Rapta, D. M. Guldi, K.-D. Asmus, K.-P. Dinse, *Magn. Reson. Chem.* **1997**, *35*, 795 – 801.
[40] S. Fukuzumi, H. Mori, T. Suenobu, H. Imahori, X. Gao, K. M. Kadish, *J. Phys. Chem. A* **2000**, *104*, 10688 – 10694.
[41] J. C. Bonner, M. E. Fisher, *Phys. Rev.* **1964**, *135*, A640 – A658.
[42] B. Gotschy, G. Völkel, *Appl. Magn. Reson.* **1996**, *11*, 229 – 238.
[43] U. Bilow, M. Jansen, *Z. Anorg. Allg. Chem.* **1995**, *621*, 982.
[44] D. V. Konarev, A.Yu. Kovalevsky, S. S. Khasanov, G. Saito, A. Otsuka, R. N. Lyubovskaya, *Eur. J. Inorg. Chem.* **2005**, 4822 – 4828.
[45] D. V. Konarev, S. S. Khasanov, E. I. Yudanova, R. N. Lyubovskaya, *Eur. J. Inorg. Chem.* **2011**, 816 – 820.
[46] D. N. Laikov, *Chem. Phys. Lett.* **1997**, *281*, 151 – 156.
[47] J. P. Perdew, K. Burke, M. Ernzerhof, *Phys. Rev. Lett.* **1996**, *77*, 3865 – 3868.
[48] G. M. Sheldrick, *Acta Crystallogr. Sect. A* **2008**, *64*, 112 – 122.

Received: December 11, 2013
Published online on March 26, 2014